α-Catenin-Vinculin Interaction Functions to Organize the Apical Junctional Complex in Epithelial Cells

Mitsuko Watabe-Uchida,* Naoshige Uchida,* Yuzo Imamura,‡ Akira Nagafuchi,‡ Kazushi Fujimoto,§ Tadashi Uemura,* Stefan Vermeulen,∥ Frans van Roy,¶ Eileen D. Adamson,** and Masatoshi Takeichi*

*Department of Biophysics, Faculty of Science, Kyoto University, Kitashirakawa, Sakyo-ku, Kyoto 606-8502; ‡Department of Cell Biology and §Department of Anatomy, Faculty of Medicine, Kyoto University, Yoshida, Sakyo-ku, Kyoto 606-8507, Japan; ∥University Hospital of Ghent and ¶Department of Molecular Biology, VIB-University of Ghent, B-9000 Ghent, Belgium; and **The Burnham Institute, La Jolla, California

Abstract. αE-catenin, a cadherin-associated protein, is required for tight junction (TJ) organization, but its role is poorly understood. We transfected an αE-catenin–deficient colon carcinoma line with a series of αE-catenin mutant constructs. The results showed that the amino acid 326–509 domain of this catenin was required to organize TJs, and its COOH-terminal domain was not essential for this process. The 326–509 internal domain was found to bind vinculin. When an NH_2-terminal αE-catenin fragment, which is by itself unable to organize the TJ, was fused with the vinculin tail, this chimeric molecule could induce TJ assembly in the αE-catenin–deficient cells. In vinculin-null F9 cells, their apical junctional organization was impaired, and this phenotype was rescued by reexpression of vinculin. These results indicate that the αE-catenin-vinculin interaction plays a role in the assembly of the apical junctional complex in epithelia.

Key words: cadherin • catenin • tight junction • vinculin • zonula adherens

Simple epithelia have a specialized junctional structure, comprising zonula occludens or tight junction (TJ),[1] zonula adherens (ZA; also called the adherens junction, intermediate junction, or belt desmosome), and desmosome at the apical area of the lateral cell–cell contacts, which is known as the junctional complex (Farquhar and Palade, 1963). TJ is located at the apical-most portion, constituting the transepithelial permeability barrier. Occludin is a transmembrane component of the TJ (Furuse et al., 1993), and is associated with ZO-1 and other cytoskeletal proteins to organize this unique junction (Furuse et al., 1994).

Just next to the TJ lies the ZA. The main adhesion receptors in the ZA are the classic cadherins (Boller et al., 1985; Takeichi, 1988), and these molecules are associated with catenins, including β-catenin and α-catenin, at the cytoplasmic domain of the former (Barth et al., 1997). These three proteins form a complex in the sequence of cadherin-to-β-catenin, and β-catenin-to-α-catenin (Barth et al., 1997). There are two subtypes of α-catenin: epithelial αE-catenin (Nagafuchi et al., 1991; Herrenknecht et al., 1991) and neural αN-catenin (Hirano et al., 1992). The αE-catenin was found to interact with actin filaments (Rimm et al., 1995), α-actinin (Nieset et al., 1997), and ZO-1 (Itoh et al., 1997), to which other catenins may also bind (Rajasekaran et al., 1996). While ZA is defined as a component of the junctional complex, the cadherin–catenin complex itself is not confined to this structure, but is distributed throughout the lateral cell–cell contacts in many epithelia. The ZA is demarcated from the other cadherin-based junctions by having a thick actin belt called the circumferential filament band (Drenckhahn and Dermietzel, 1988), and also by enrichment of some cytoskeletal proteins. Vinculin is one such protein accumulated in ZA (Geiger et al., 1980; Geiger et al., 1981; Yonemura et al., 1995). α-Actinin is another protein concentrated in ZA (Geiger et al., 1979; Craig and Pardo, 1979), although it is more broadly distributed than vinculin along the lateral cell membranes (Geiger et al., 1981). Some other novel proteins were recently identified as ZA components (Mandai et al., 1997; Yamamoto et al., 1997). The desmosome, another type of cadherin-mediated junction (Buxton and Magee, 1992), is located below the ZA, and is associated with the intermediate filaments. These three junctional structures are typi-

1. *Abbreviations used in this paper*: GST, glutathione S-transferase; MBP, maltose-binding proteins; pAb, polyclonal antibody; TJ, tight junction; ZA, zonula adherens.

cally aligned in this order in the simple epithelia, although desmosomes are also independently distributed in other areas of the cell membrane. Little is known about the mechanism of how such polarized junctional arrangement can be established.

The close positional relation between TJ and ZA suggests their molecular reciprocal interaction. Previous studies indeed indicated that the cadherin-mediated adhesion is a prerequisite for TJ formation. Incubation of cells with cadherin-blocking antibodies disrupts the TJ structure and function (Gumbiner and Simons, 1986; Gumbiner et al., 1988). Cells whose αE-catenin gene is deleted cannot form TJs (Watabe et al., 1994). These observations strongly suggest that TJ formation is governed by cadherin-mediated adhesion.

The present study aimed to understand the molecular roles of αE-catenin in epithelial junctional complex formation. As mentioned above, αE-catenin–deficient cell lines cannot establish the junctional complex. Sublines of the human colon carcinoma DLD-1 are deficient in αE-catenin expression (van Hengel et al., 1997). We used one of these sublines to introduce a series of αE-catenin mutant molecules, and found that an internal domain of αE-catenin is essential for TJ organization. Notably, this domain was found to interact with vinculin, and further analysis provided evidence that the αE-catenin–vinculin interaction is crucial for TJ assembly. Furthermore, vinculin null mutation impaired the apical junctional organization in F9 cells. Therefore, we could uncover a role for vinculin in cell–cell junctional organization that had long been sought via functional analysis of αE-catenin. We discuss how the αE-catenin–vinculin interaction regulates junctional complex formation.

Materials and Methods

Molecular Construction

αE-Catenin expression vectors carrying the T7 epitope at their carboxyl end were constructed as follows: part of pPET-3c encoding the T7 epitope (Novagen, Inc., Madison, WI) was inserted into pBluescript, which was cut and blunted at BamHI sites and self-ligated for introduction of a stop codon (pBT7-stop). The expression vectors for mouse αE-catenin cDNA, pBAT-α-T7, and its deletion mutants, pBAT-αΔ-T7s, were constructed by shuttling restriction fragments of pBAT-α (Watabe et al., 1994) into pBT7-stop and substituting them for the αE-catenin–coding region of pBAT-α. For isolation of mouse vinculin cDNA, a fragment of vinculin cDNA was obtained by RT-PCR, and was used to screen a lambda ZAP oligo dT-primed cDNA library of mouse F9 cells. One vinculin cDNA clone, Vin-c-3, which covers the entire coding region, was obtained. αE-Catenin/vinculin chimeras, αE/vinHead, and αE/vinTail, were constructed by shuttling the fragments of Vin-c-3 encoding amino acids 1–823 and 822–1067 into pBT7-stop, respectively, and inserting these constructs into pBAT-α, which was cut leaving the region encoding amino acids 1–325 of αE-catenin.

Vectors encoding fusion proteins between glutathione S-transferase (GST) and parts of αE-catenin, or between maltose-binding proteins (MBP) and parts of vinculin were constructed for in vitro binding assay. αE-Catenin or vinculin fragments were constructed by PCR amplification of selected regions of pBAT-α-T7, pBAT-α(1–325/510–890)-T7, or Vin-c-3 by use of primers incorporating EcoRI restriction sites. The obtained amplicons were inserted into pGEX-1λT (Pharmacia Biotechv Sverige, Uppsala, Sweden) or pMAL™-cRI (New England Biolabs Inc., Beverly, MA).

Cells and cDNA Transfection

Human colon carcinoma DLD-1 (Dexter et al., 1979) cells were cultured in a 1:1 mixture of DMEM and Ham's F12 supplemented with 10% FCS (DH10). DLD-1/R2 was obtained by cloning a round variant from DLD-1 (Vermeulen et al., 1995), and DLD-1/R2/7 was a subclone of DLD-1/R2. F9, γ227, γ229, R3, and R15 cells were also cultured in the above medium.

To enhance spreading of these cells, particularly vinculin-null cells, collagen-coated coverslips were used. The culture medium was replaced twice a day for F9 and its derivatives.

These cells were transfected by electroporation. Trypsinized cells (1×10^6) were suspended in 200 µl of Hepes-buffered (pH 7.4) Ca^{2+}- and Mg^{2+}-free saline. 20 µg of an expression vector and 2 µg of pSV2 hph (Gritz and Davies, 1983; Sugden et al., 1985) were added to the suspension, which was electrified at 960 µF, 200 V. The cells were selected in hygromycin-containing medium. Isolated hygromycin-resistant cell clones were tested for their expression of transfected molecules by immunofluorescence and immunoblotting.

Antibodies

The following antibodies were used: rabbit polyclonal antibody (pAb) against mouse E-cadherin; mouse mAbs HECD-1 (Shimoyama et al., 1989) and SHE78-7 (Takara Shuzo Co., Ltd., Shiga, Japan) to E-cadherin; rat mAb ECCD-2 to E-cadherin (Shirayoshi et al., 1986); rabbit pAb to β-catenin (Shibamoto et al., 1994); mouse mAb 5H10 to β-catenin (Uchida et al., 1996); rat mAb α18 to αE-catenin (Nagafuchi and Tsukita, 1994); mouse mAb T7. Tag™ Antibody (Novagen, Inc.); rabbit pAb to ZO-1 (Zymed Labs., Inc., S. San Francisco, CA); mouse mAb MOC37 to occludin (Saitou et al., 1997); mouse mAbs VIN-11-5 and hVIN-1 to vinculin (Sigma Chemical Co., St. Louis, MO); mouse mAb BM-75.2 to α-actinin (Sigma Chemical Co.); rabbit pAb to spectrin (Seikagaku Corp., Tokyo, Japan); and rabbit pAb to MBP (New England Biolabs, Inc., Beverly, MA). For detection of primary antibodies, we used biotinylated antibodies, FITC-linked streptavidin, Texas red–linked streptavidin, FITC-labeled antibodies, Texas red–labeled antibodies, and HRP-conjugated antibodies. FITC-labeled phalloidin (Molecular Probes, Inc., Eugene, OR) was used for detection of F-actin.

Immunofluorescence Staining

Before fixation, cells were cultured on coverslips for 2 d. They were fixed by one of the following methods: (a) for staining for α-actinin, cells were fixed and permeabilized by treatment with methanol on ice for 5 min. Methanol was gradually replaced with water by incubating cells with 75, 50, and 25% methanol in water for 2 min each; (b) for staining for F-actin, cells were fixed with 3.5% paraformaldehyde in Hepes-buffered (pH 7.4) saline with 1 mM Ca^{2+} and Mg^{2+} (HBSS) at 4°C for 20 min, and were permeabilized by acetone treatment at −20°C for 10 min; (c) for staining for other molecules, cells were treated as above, or were fixed with 3.5% paraformaldehyde in HBSS at 4°C for 20 min and permeabilized by treatment with methanol at −20°C for 20 min. Double-immunofluorescence staining was carried out as described previously (Watabe et al., 1994). The immunostained samples were examined under an Axiophot (Carl Zeiss Inc., Thornwood, NY) or an MRC-1024confocal microscope (Bio-Rad Laboratories, Hercules, CA). Confocal pictures were taken to show optical x-y sections.

Immunoprecipitation and Immunoblotting

All steps in the following immunoprecipitation protocol were carried out either on ice or at 4°C. Cells were scraped out of dishes with a rubber policeman, and were dissolved in the extraction buffer consisting of 1% NP-40, 1% Triton X-100, 1 mM $CaCl_2$, and 1 mM PMSF in TBS (see below). After incubation for 30 min, the extracts were centrifuged at 100,000 g for 10 min. The supernatants were mixed with Sepharose 4B–conjugated secondary antibodies that had been preincubated with primary antibodies. Sepharose-arrested proteins were boiled in the Laemmli sample buffer, and were resolved by SDS-PAGE as previously described (Watabe et al., 1994).

In Vitro Protein-binding Assay

GST fusion proteins were expressed in *Escherichia coli* DH5α, and the cells cultured in 250 ml of culture medium were collected and lysed in 15 ml of TBS (50 mM Tris-HCl, 150 mM NaCl, pH 7.6) containing 1% EDTA and 1 mM PMSF (TBS-EDTA) by use of a sonicator. The sonicates were centrifuged at 27,000 g for 10 min, and then at 100,000 g for 10 min. The resulting supernatant was incubated with 100 µl of glutathione-Sepharose 4B for 1 h, and the Sepharose beads were washed three times with TBS-EDTA for 5 min.

E19-20 chicken gizzards were homogenized in TBS-EDTA in a Dounce homogenizer (one gizzard/15 ml TBS-EDTA). The lysate was centrifuged at 27,000 g for 10 min, and subsequently at 100,000 g for 10

min. The supernatant derived from one gizzard was mixed for 1 h with 100 μl of the above Sepharose-bound GST fusion proteins, and then the Sepharose beads were washed five times with 500 mM NaCl in TBS-EDTA for 5 min. For examination of direct association between GST- and MBP-fusion proteins, the MBP fusion proteins were collected in the same way as described for GST fusion proteins. 2 ml of the MBP fusion protein solution was mixed with 50 μl of the above Sepharose-bound GST fusion proteins. For release of the materials bound to the Sepharose beads, the latter were boiled with SDS, as described above.

Cell Aggregation Assay

Cells were completely dissociated into single cells by TE-treatment (Takeichi, 1977), and 1×10^5 cells were placed into each well of a 24-well multidish (Nunc Inc., Roskilde, Denmark) containing 500 μl of DH10, whose bottom had be precoated with 50 μl of 1% agar. The cells were left undisturbed in a CO_2 incubator at 37°C for 1 d, and the morphology of cell aggregates formed were observed under a Diaphot microscope (Nikon, Inc., Melville, NY).

Electron Microscopy

Freeze-fracture EM was done by conventional methods. For ultrathin-section EM, cells were cultured in plastic dishes and processed by a conventional method (Uchida et al., 1996), except that cell sheets were peeled off immediately after adding propylene oxide.

Results

Aberrant Cell–Cell Junctions in the Absence of αE-Catenin

DLD-1 is a colon carcinoma line with typical epithelial organization. DLD-1/R2/7, a subclone of DLD-1, showed a normal level of E-cadherin and β-catenin, but had no αE-catenin protein expression (Fig. 1 A); the genetic background of this defect will be published elsewhere. The DLD-1/R2/7 line, abbreviated to R2/7, formed epithelioid clusters, but their intercellular associations were apparently loose (Fig. 1 C) compared with those of the parent DLD-1 colonies (Fig. 1 B). When R2/7 cells were transfected with αE-catenin cDNA, the original tightly associated epithelial morphology was restored (Fig. 1 D). As these αE-catenin transfectants were indistinguishable from the parent DLD-1, one of their clones, R2/7-αE, was used as a representative line of the normal cells throughout subsequent experiments.

To determine how the loss of αE-catenin affects junctional organization, we compared R2/7 and R2/7-αE for their expression of various junctional proteins. Double-immunostaining for E-cadherin and ZO-1, a component of the tight junction (TJ), showed that in R2/7-αE, these molecules were localized at cell–cell boundaries in the pattern typical for many simple epithelia: ZO-1 was confined at the most apical portion of cell–cell contacts, displaying a honeycomb-like distribution pattern (Fig. 1 E). E-cadherin was more broadly distributed at the lateral cell–cell boundaries, and its apical edge coincided with the ZO-1 staining (Fig. 1 H). On the other hand, in R2/7, ZO-1 was accumulated in a circular or patchy pattern on the top surface, never showing the honeycomb pattern (Fig. 1 F); and it was rarely localized in the lateral membranes (Fig. 1 G). E-cadherin was detected in two separate positions, one along the ZO-1-positive rings (Fig. 1 I) and the other at portions of the lateral membrane (Fig. 1 J). The latter E-cadherin signals were condensed at cell-cell contact sites, being little associated with ZO-1 (Fig. 1, G and J).

The ZO-1–positive rings on the top surface of R2/7 cells were also delineated by staining for actin (Fig. 1, P and Q), occludin (Fig. 1 R), and α-actinin (Fig. 1 S). By contrast, vinculin was never localized along the ZO-1 rings (Fig. 1 T) nor at the lateral cell–cell contact sites in the R2/7 cells (Fig. 4 D). In R2/7-αE, on the other hand, all these junctional proteins were accumulated together at the apical cell–cell boundaries (Fig. 1 K–O), coinciding with the apical signals of E-cadherin. In addition, E-cadherin was always colocalized with β-catenin at cell–cell boundaries, and also coimmunoprecipitated with this catenin from both cell lines (data not shown), supporting the widely accepted view that they form a direct molecular complex.

The above observations suggested that TJs were disorganized by the loss of αE-catenin. To further examine this point, the above cells were analyzed by a freeze-fracture replica method. In R2/7-αE, typical TJ strands arranged into a mesh-like pattern were detected (Fig. 1 U). Unexpectedly, even in R2/7 cells similar structures were found, although they were discontinuous and patchy (Fig. 1 V), suggesting that local TJ formation occurs in these cells. As described later, R2/7 cells are connected with neighbors through filopodial processes at marginal areas of their apical surface (Fig. 7 I); these contact points could serve as sites for such discontinuous TJ formation. These findings indicate that the loss of αE-catenin did not block TJ formation per se, but abolished its network-type organization.

Amino Acid Residues 326–509 of αE-Catenin are Necessary for Organization of the ZO-1 Network

To determine the domains of αE-catenin necessary for TJ assembly, we generated a series of its deletion mutants, tagged with T7 at their COOH terminus (Fig. 2 A). These were introduced into R2/7 cells, and subsequently multiple transfectant clones were isolated for each construct, among which a representative clone was chosen for the following experiments. Each clone expressed a protein with the expected size (Fig. 2 B). From lysates of these clones, antibodies to the T7 tag coimmunoprecipitated E-cadherin only when the αE-catenin constructs contained the NH_2-terminus (Fig. 2 C), consistent with the finding that the NH_2-terminal region of α-catenin is required for its association with β-catenin (Bullions et al., 1997; Nieset et al., 1997; Obama and Ozawa, 1997; Sehgal et al., 1997).

Cells expressing the above mutant αE-catenin molecules were stained for ZO-1 to assess their TJ organization. αE(1–509) in which the COOH-terminal 397 residues had been truncated induced the formation of the typical honeycomb ZO-1 network (Fig. 3 D). However, αE(1–325) with a longer COOH-terminal deletion failed to reorganize the ZO-1 distribution (Fig. 3 E). These observations suggest that residues 326–509 are important for ZO-1 organization. Consistently, cells expressing αE(1–325/510–890), in which the 326–509 portion was deleted but the other regions were left intact, could not redistribute ZO-1 (Fig. 3 F), although ZO-1 tended to be more frequently condensed at cell–cell contact sites in these transfectants than in R2/7 cells. E-cadherin was redistributed into a normal pattern with αE(1–509), but not with αE(1–325) or αE(1–325/510–890; Fig. 3, G–I). By phase-contrast microscopy, αE(1–509) cells showed tighter cell–cell associations than the other transfectants (Fig. 3, A–C). The mutant αE-catenins lacking the β-catenin–bind-
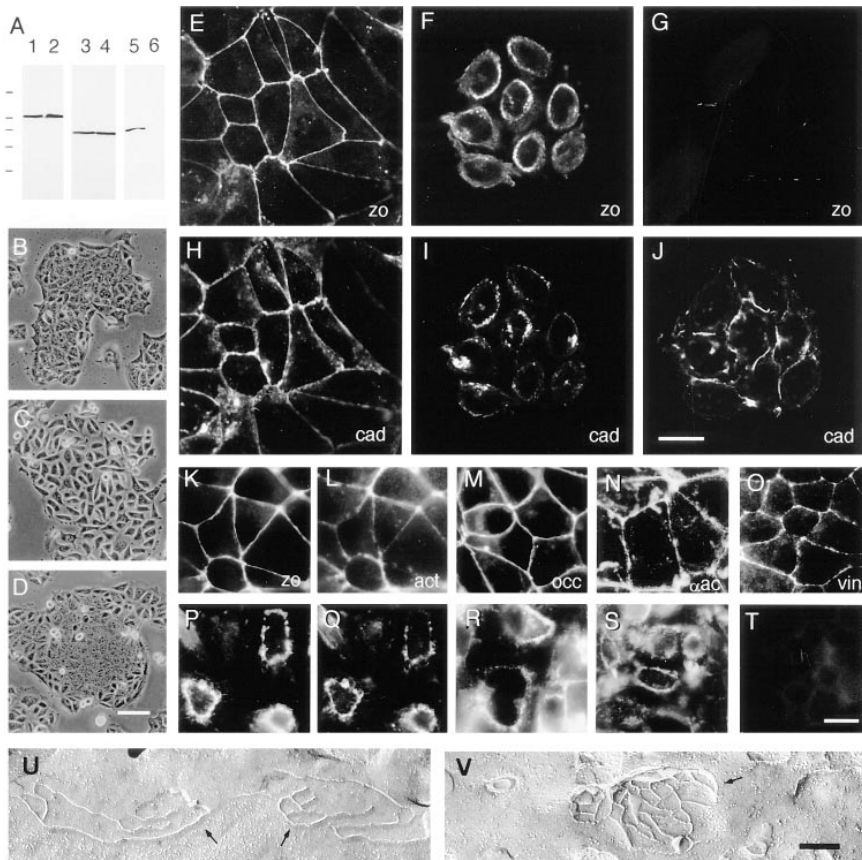
Figure 1. Junctional organization in DLD-1, R2/7, and R2/7-αE cells. (*A*) Immunoblot analysis for E-cadherin (lanes *1* and *2*), β-catenin (lanes *3* and *4*), and αE-catenin (lanes *5* and *6*) in DLD-1 (lanes *1, 3,* and *5*) or in DLD-1/R2/7 (lanes *2, 4,* and *6*). Molecular weight markers are 200, 116, 97, 66, and 45×10^3. (*B–D*) Phase-contrast micrographs of DLD-1 (*B*), R2/7 (*C*), and R2/7-αE (*D*). (*E–J*) Confocal images of double immuno-fluorescence staining for ZO-1 (*E–G*) and E-cadherin (*H–J*). (*E, H*) R2/7-αE. The focus was adjusted to an apical plane. (*F, G, I,* and *J*) R2/7. The focus was adjusted to two planes: apical (*F, I*) and middle (*G, J*). (*K–T*) Immunofluorescence staining for junctional or cytoskeletal proteins in R2/7-αE (*K–O*) and R2/7 (*P–T*). The focus was adjusted to their apical planes. Cells were double-stained for ZO-1/F-actin in *K* and *L* and in *P* and *Q*, and were singly stained for occludin (*M, R*), α-actinin (*N, S*), or vinculin (*O, T*). (*U, V*) Freeze-fracture replica views of R2/7-αE (*U*) and R2/7 (*V*) at junctional areas. TJ strands (*arrows*) are detected not only in *U* but also in *V*. zo, ZO-1; cad, E-cadherin; act, actin; occ, occludin; αac, α-actinin; vin, vinculin. These abbreviations are also used in other figures. Bars: (*B–D*) 100 μm; (*E–J* and *K–T*) 20 μm; (*U* and *V*) 200 nm.

ing domain had no effect on ZO-1 assembly. The staining pattern of occludin was identical to that of ZO-1 in all the above cell lines (data not shown).

Interaction of Vinculin with aE-Catenin at the 326–509 Domain

As a step to investigate the role of the 326–509 domain, we examined the localization of various proteins in the above series of αE-catenin transfectants that are known to be associated with the junctional complex. As mentioned al-

ready, vinculin was completely absent from the top to lateral surfaces in R2/7 cells, not colocalizing with E-cadherin (Fig. 1 *T* and Fig. 4, *A* and *D*), although it was normally located at focal adhesion sites to the substratum (data not shown). However, when the cells expressed the full-length αE-catenin, vinculin was redistributed to cell–cell boundaries to colocalize with the apical-most signals of E-cadherin (Fig. 4, *B* and *E*); the same colocalization was induced by expression of αE(1–509) (Fig. 4, *C* and *F*). The vinculin distribution was sharp, and was restricted to the apical level of cell–cell contacts close to the ZO-1 localiza-
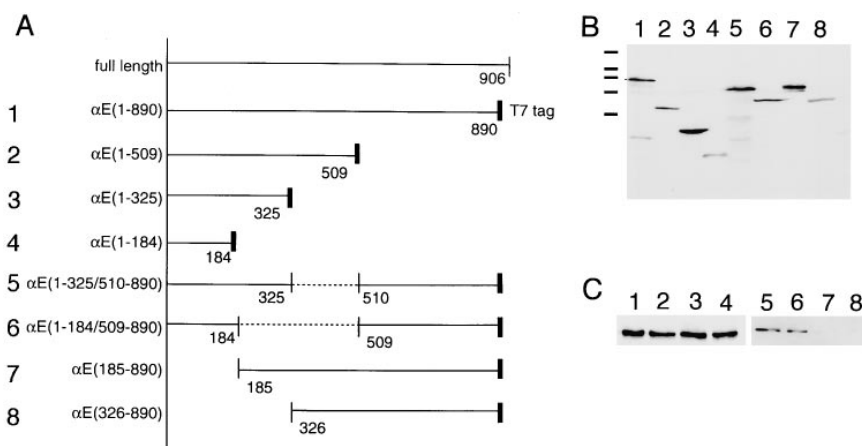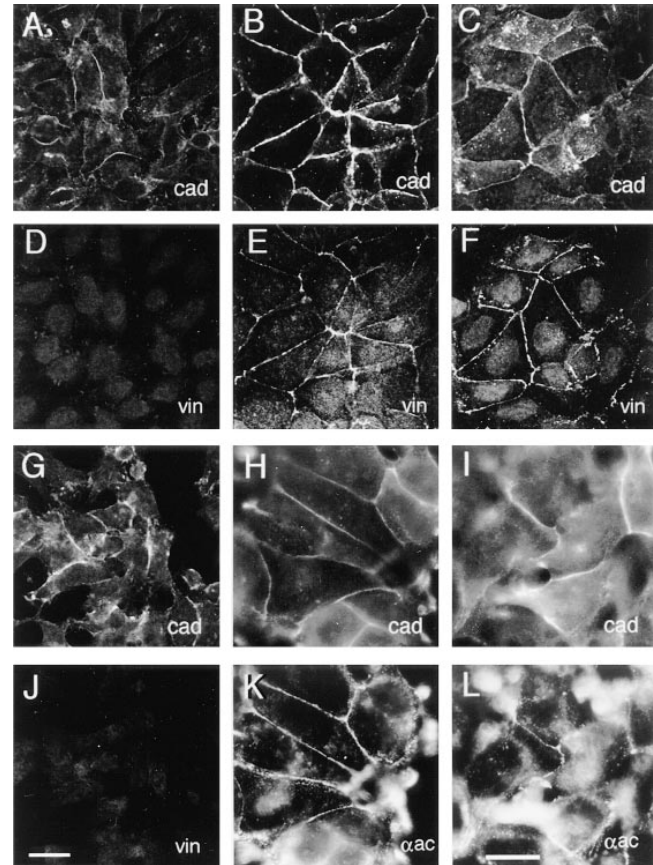

Figure 2. Deletion constructs of αE-catenin and their characterization. (*A*) Schematic drawing of the mutant αE-catenin constructs, designated as 1–8, introduced into R2/7 cells. Stable transfectants were isolated for each construct. (*B*) Immunoblot detection of the mutant αE-catenin proteins (*1–8*) expressed by the transfectants with anti-T7 tag antibodies. (*C*) Immunoblot detection of E-cadherin coimmunoprecipitated with the mutant αE-catenin molecules. Materials immunoprecipitated with an anti-T7 tag antibody from a lysate of each transfectant were subjected to detection of E-cadherin. The numbers marking the lanes in *B* and *C* correspond to the construct number in *A*. Lower bands seen in some lanes are likely degradation products of the original molecule. Positions of molecular markers are the same as in Fig. 1 *A*.

αE(1-509)   αE(1-325)   αE(1-325/510-890)
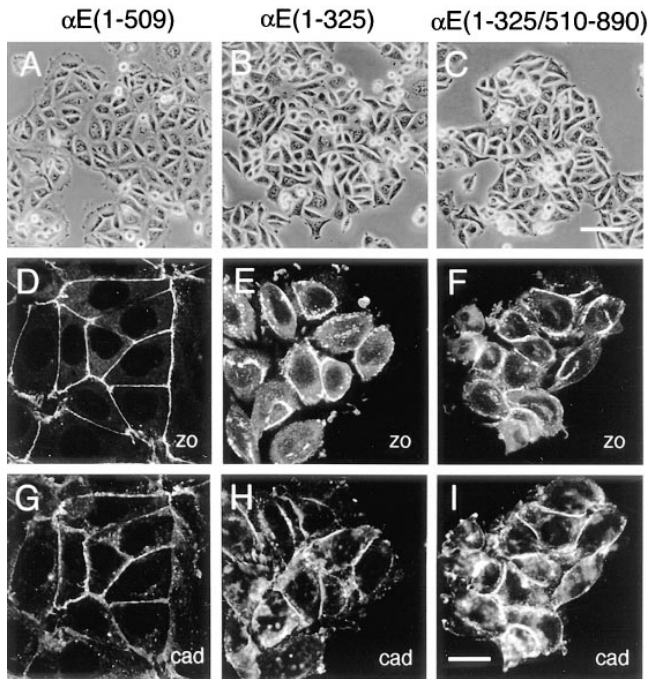
Figure 3. Only αE(1–509) can rescue R2/7 cells to organize the TJ. (*A*, *D*, and *G*) R2/7-αE(1–509). (*B*, *E*, and *H*) R2/7-αE(1–325). (*C*, *F*, and *I*) R2/7-αE(1–325/510–890). (*A–C*) Phase-contrast micrographs of cells expressing these mutant αE-catenins. (*D–I*) Confocal images of double immunofluorescence staining for ZO-1 (*D–F*) and E-cadherin (*G–I*). Bars: (*A–C*) 100 μm; (*D–I*) 20 μm.

Figure 4. Colocalization of vinculin or α-actinin with E-cadherin. (*A* and *D*) R2/7; (*B* and *E*) R2/7-αE; (*C* and *F*; *H* and *K*) R2/7-αE(1–509). (*G* and *J*; *I* and *L*) R2/7-αE(1–325/510–890). Double immunofluorescence staining for E-cadherin and vinculin (*A* and *D*; *B* and *E*; *C* and *F*; *G* and *J*), and for E-cadherin and α-actinin (*H* and *K*; *I* and *L*). *A–G* and *J* are confocal images. Bars: (*A–G* and *J*; *H*, *I*, *K*, and *L*) 20 μm.

tion (data not shown), as observed for many normal epithelial cells (e.g., Yonemura et al., 1995). All other constructs lacking the 326–509 domain, including αE(1–325/510–890), never led vinculin to colocalize with E-cadherin (Fig. 4, *G* and *J*). These results suggest that the 326–509 region of αE-catenin plays a role in attracting vinculin to the E-cadherin–positive cell–cell contacts. Vinculin localization at the focal adhesion sites appeared to be normal in all the transfectant lines. α-Actinin also codistributed with E-cadherin in the αE(1–509) cells (Fig. 4, *H* and *K*). However, this protein sporadically colocalized with E-cadherin, even in cells expressing the αE-catenin without the 326–509 domain, such as αE(1–325/510–890) (Fig. 4, *I* and *L*), indicating no consistent correlation between the α-actinin/E-cadherin codistribution and the presence of the 326–509 domain. As far as examined, vinculin was the only protein that responded to the presence or absence of the 326–509 domain in its redistribution to the apical cell–cell contact sites, although other unidentified proteins could show similar behavior.

For more direct identification of molecules that can associate with the 326–509 domain, we generated GST-αE-catenin fusion proteins having the 1–325 or 1–509 domain (Fig. 5 *A*, *2* and *3*), and incubated them with chick gizzard lysates as a source of cytoskeletal proteins. SDS-PAGE analysis of the bound materials revealed that the 1–509 construct precipitated two major proteins that migrated to the 130–120 kD region, but the other construct did not (Fig. 5 *B*; *top, arrowheads*). In Western blotting, both bands reacted with antibodies to vinculin (Fig. 5 *B*;

middle, arrowheads), suggesting that they are two variant forms of vinculin: metavinculin, and vinculin (Molony and Burridge, 1985). As controls, we found that β-catenin was copurified with both constructs as expected, but α-actinin and spectrin were not associated with either construct (Fig. 5 *B*, *bottom*). These findings indicate that the 326–509 domain is involved in the association of αE-catenin with vinculin, consistent with the above immunostaining results. No other proteins were copurified specifically with this domain; at least as major components, as judged by silver staining of the above electrophoretic samples.

To test if the association of αE-catenin with vinculin is mediated by their direct binding, we constructed other GST-αE–catenin mutant molecules (Fig. 5 *A*), including a molecule consisting of only the 326–509 domain, and subjected them to assays of their ability to bind the head domain or tail domain of vinculin constructed as MBP-fusion proteins (Fig. 5 *A*). The vinculin head domain (MBP-vin-Head) bound not only the intact αE-catenin, but also to αE(1–509) and αE(326–509) (Fig. 5 *C*, *vinH*); it did not bind any other constructs lacking the 325–509 domain of αE-catenin. On the other hand, the tail domain of vinculin (MBP-vinTail) reacted with none of the αE-catenin con-
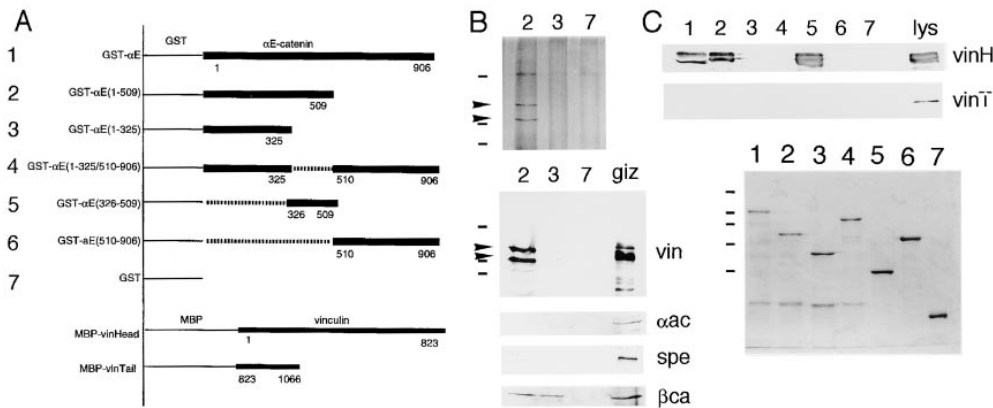
Figure 5. In vitro binding of vinculin with αE-catenin. (*A*) Schematic drawing of GST-αE-catenin fusion proteins (*1–7*), and of MBP-vinculin fusion proteins (MBP-vinHead and MBP-vinTail). (*B*) Detection of proteins bound to the GST-αE-catenin fusion proteins 2, 3, and 7 (*control*) that had been incubated with chicken gizzard extracts. (*Top*) proteins bound to the GST-fusion proteins were separated by SDS-PAGE, and were visualized by silver staining. Two bands of 130 and 120 kD (*arrowheads*) were precipitated with GST-αE(1–509) (*2*), but not with the other constructs. These bands were recognized with anti-vinculin antibodies (*middle*). α-Actinin and spectrin did not bind to any of these constructs, whereas β-catenin was precipitated with 2 as well as with 3 (*bottom*). giz, the original extract of gizzards used for these binding assays; vin, vinculin; αac, α-actinin; spe, spectrin; βca, β-catenin. Positions of molecular markers are 200, 116, and 97 × 10³. (*C*) Binding of MBP-vinHead (*vinH*) or MBP-vinTail (*vinT*) to GST-αE-catenin fusion proteins 1–7. Sepharose beads conjugated with these GST-fusion proteins were incubated with a lysate of *E. coli* expressing the MBP-fusion proteins. Coprecipitated proteins were analyzed by Western blotting with antibodies to vinculin (for MBP-vinHead) or to MBP (for MBP-vinTail; *top*). Each sample for electrophoresis contained an equal molar amount of the GST-fusion proteins that had been adjusted before loading on the gel. (*Bottom*) Coomassie blue staining for the GST-αE-catenin fusion proteins 1–7 conjugated to Sepharose beads. Positions of molecular markers are the same as in Fig. 1 *A*. lys, the original lysate of *E. coli* used for this binding assay.

structs (Fig. 5 *C*, *vinT*). All these results indicate that αE-catenin can directly bind to the head domain of vinculin at the 326–509 domain. We also examined if E-cadherin could be copurified with vinculin by immunoprecipitation, but the results were negative as previously observed (Knudsen et al., 1995; Tsukatani et al., 1997; Hazan et al., 1997). It is possible that the E-cadherin/αE-catenin/vinculin complex was not soluble to our detergent solutions, as we found that their colocalization was still detected in the cells extracted with nonionic detergents. Alternatively, their association might have been disrupted during the detergent extraction; it is of note that the above in vitro binding assays were carried out under detergent-free conditions.
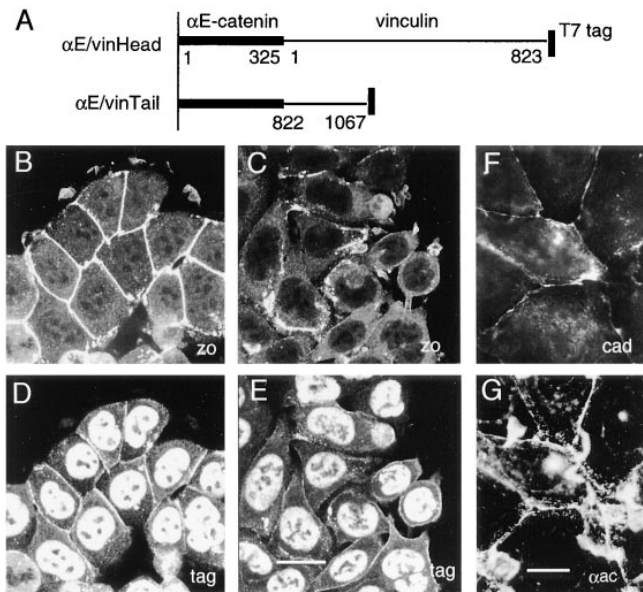
αE-Catenin-Vinculin Chimeric Proteins Can Induce the ZO-1 Network

As found above, the activity of αE-catenin to organize the ZO-1 network was correlated with its ability to bind vinculin. This finding suggests that the ZO-1–organizing activity of αE-catenin could be mediated by vinculin itself. To test this idea, we constructed cDNAs encoding the 1–325 αE-catenin fragment whose COOH terminus was fused with the head (αE/vinHead) or tail (αE/vinTail) domain of vinculin (Fig. 6 *A*), and these constructs were introduced into R2/7 cells to isolate transfectants. The 1–325 αE-catenin fragment by itself cannot redistribute ZO-1, as mentioned above. Both chimeric proteins were found to bind the E-cadherin/β-catenin complex (data not shown). When αE/vinTail was expressed, ZO-1 was redistributed to exhibit a honeycomb pattern (Fig. 6 *B*), colocalizing with E-cadherin or tag signals (Fig. 6 *D*). On the other hand, αE/vinHead expression could not reorganize the ZO-1 distribution (Fig. 6, *C* and *E*). These results suggest that the tail domain of vinculin, associated with αE-catenin, plays a role in ZO-1 organization. Incidentally, in the αE/vinTail-

expressing cells, α-actinin did colocalize with E-cadherin or αE/vinTail (Fig. 6, *F* and *G*) despite the absence of the identified α-actinin–binding sites in this chimeric protein, which are amino acids 325–394 in αE-catenin (Nieset et al., 1997) and amino acids 1–107 in vinculin (Kroemker et al., 1994). Therefore, the α-actinin/E-cadherin colocalization often observed during this study does not necessarily suggest that they are forming a molecular complex.

### Morphological Assessment of Functions of Different αE-Catenin Domains

To gain further insight into the role of different domains of αE-catenin, we analyzed the junctional structures of cells expressing various αE-catenin constructs by EM. R2/7-αE cells formed monolayer sheets with a smooth surface in which individual cells were essentially of cuboidal shape and closely associated with each other at their lateral membranes (Fig. 7 *A*). At the apical-most portion of their lateral contacts, the junctional complexes were observed (Fig. 7 *D*). The ZA was not always clearly detectable as a domain separable from the TJ, suggesting that these two junctions might be fused to each other. Similar apical junctional structures were observed in cells expressing αE(1–509) (Fig. 7 *E*) and αE/vinTail (Fig. 7 *F*). Despite such relatively normal organization of the apical junctional complexes, these cells differed from R2/7-αE cells in their overall association patterns. Cells with αE(1–509) tend to overlap each other at their basolateral regions (Fig. 7 *B*), suggesting that their adhesive interaction was not perfectly controlled at the nonapical lateral membranes. In the case of αE/vinTail-expressing cells, their intercellular contacts were limited to the areas with the apical junctional complex and desmosomes; large intercellular spaces were formed at the sites where these junctional structures were absent (Fig. 7, *C* and *F*).

Figure 6. An αE-catenin/vinculin chimeric protein can redistribute ZO-1. (*A*) Schematic drawing of αE-catenin/vinculin chimeric proteins. The NH_2-terminal 1–325 amino acid domain was fused with the NH_2-terminal 1–823 or COOH-terminal 822–1067 domain of vinculin. (*B* and *D*) Double immunofluorescence staining for ZO-1 (*B*) and T7 tag (*D*) of cells expressing αE/vinTail. (*C* and *E*) Double immunofluorescence staining for ZO-1 (*C*) and T7 tag (*E*) of cells expressing αE/vinHead. (*F* and *G*) Double immunofluorescence staining for E-cadherin (*F*) and α-actinin (*G*) in cells expressing αE/vinTail. Staining signals observed in the nuclei are due to nonspecific association of the anti-T7 tag antibodies with these structures. Bars (*B–E; F* and *G*), 10 μm.

On the other hand, in R2/7 cells no typical junctional complex was observed (Fig. 7 *I*); their plasma membranes were simply apposed to each other with an occasional presence of desmosomes, and in some cells the apical-most portion of the lateral contacts was occupied by a desmosome instead of the junctional complex (Fig. 7 *I, insert*). Interestingly, these cells extended filopodia from marginal areas of their apical surface, and formed spotty contacts with neighboring cells at similar areas. At these contact sites, electron-dense junction-like structures were observed (Fig. 7 *I, arrowheads*). Also, in cells expressing αE(1–325), αE(1–184), αE(1–326/509–890) (Fig. 7 *J*), and αE/vinHead, no apical junctional complexes were found. As an overall view, these cells that are unable to form the apical junctional complex exhibited very irregular patterns of intercellular association (Fig. 7, *G* and *H*).

We then attempted to estimate the E-cadherin–mediated aggregating activity of cells expressing different αE-catenin constructs. An ideal experiment to this end is to measure the rate of reaggregation of cells that have been dissociated with preservation of their cadherins by the trypsin-Ca^{2+}-treatment method (Takeichi, 1977; Takeichi, 1988). However, DLD-1 cells were difficult to dissociate into single cells by this method. We therefore carried out the following assay: cells were dissociated into single cells by a trypsin–EDTA treatment, and were incubated overnight to induce cell reaggregation in the absence or presence of E-cadherin–blocking antibodies. Without the anti-
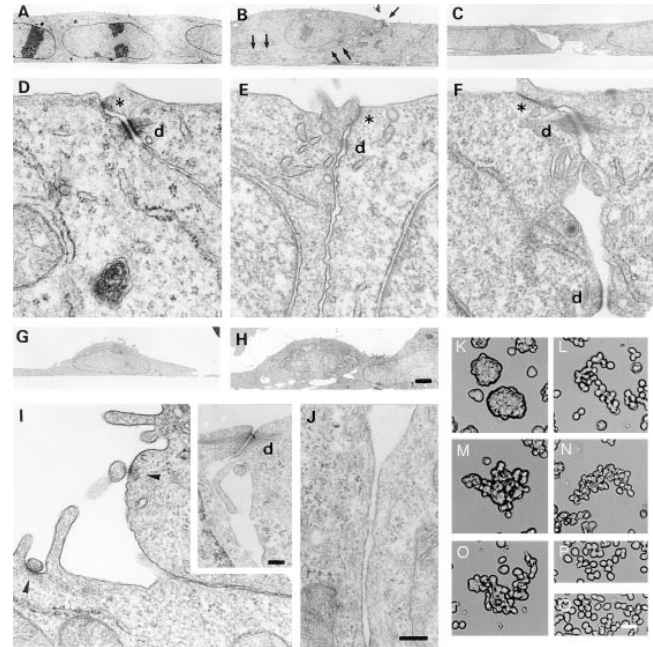
Figure 7. Association pattern of cells expressing various αE-catenin constructs. (*A–J*) Vertical EM sections of cells in monolayer cultures seen at a low magnification (*A–C, G* and *H*), and their close-up views at apical cell–cell junction areas (*D–F, I* and *J*). (*A* and *D*) R2/7-αE. (*B* and *E*) R2/7-αE(1–509). (*C* and *F*) R2/7-αE/vinTail. (*G* and *I*) R2/7. (*H* and *J*) R2/7-αE(1–325/510–890). Insert in I is another section of R2/7, showing a desmosome at the apical-most junction. Arrows in *B* point to a boundary between two cells that irregularly overlap each other. Asterisks indicate TJ-ZA complexes. Arrowheads in *I* point to filopodial contacts with electron-dense cytoplasmic materials. d, desmosome. (*K–Q*) Aggregates of R2/7 cells and their αE-catenin transfectants in the absence (*K–O*) or presence (*P* and *Q*) of anti-E-cadherin antibodies. (*K* and *P*) R2/7-αE. (*L* and *Q*) R2/7. (*M*) R2/7-αE(1–509). (*N*) R2/7-αE(1–325/510–890). (*O*) R2/7-αE/vinTail. Cells were trypsinized into single cells and cultured overnight in agar-coated dishes. Bars: (*A–C, G,* and *H*) 2 μm; (*D–F, I* and *J*) 200 nm; (*K–Q*) 20 μm.

bodies, R2/7-αE cells formed compact aggregates in which cells were tightly packed (Fig. 7 *K*), whereas with the blocking antibodies, the cells remained single or formed only loose clusters (Fig. 7 *P*). In contrast to R2/7-αE ones, R2/7 cells loosely aggregated, and their aggregates were never compacted (Fig. 7 *L*), although this aggregation was still sensitive to the anti–E-cadherin antibodies, as the cells were further dispersed by the antibodies (Fig. 7 *Q*). Aggregates of cells with αE(1–509) (Fig. 7 *M*) or αE/vinTail (Fig. 7 *O*) exhibited a morphology intermediate to that of the above cases; they were partly compacted, although the latter aggregates tended to be less compacted. The aggregation profile of the cells expressing αE(1–325), αE(1–184), αE(1–325/510–890), and αE/vinHead was essentially identical to that of R2/7, although those with αE(1–325/510–890) were slightly more adhesive than the others (Fig. 7 *N*). To summarize, the activity of αE-catenin to induce compacted aggregates was expressed in the following order: intact αE-catenin > αE(1–509) ≥ αE/vinTail > αE(1–

$325/510–890) \geq \alpha E(1–325) = \alpha E(1–184) = \alpha E/vinHead =$ no αE-catenin.

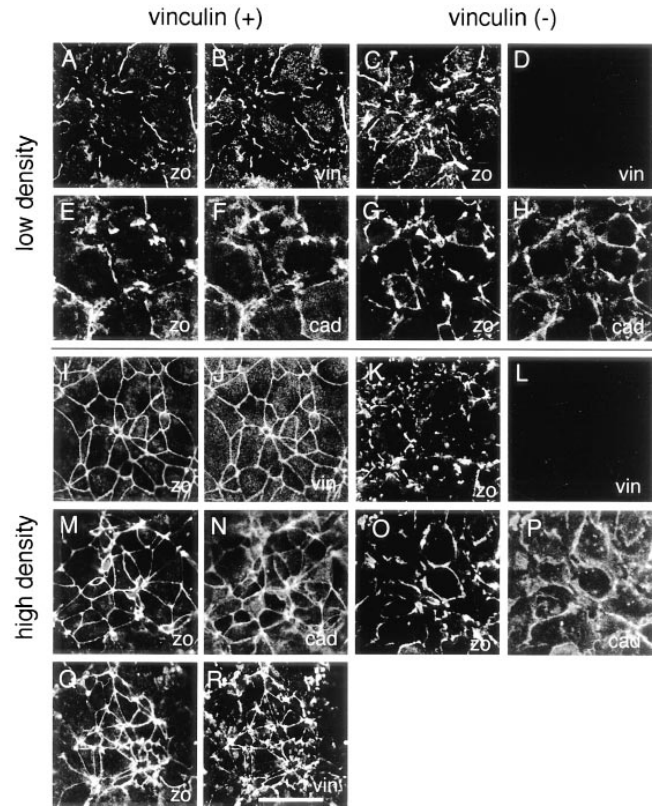## Apical Junctional Organization in Vinculin-deficient Cells

Finally, to confirm the importance of vinculin in cell–cell junction formation, we examined junctional organization in two independent sublines of F9 embryonal carcinoma cells—γ227 and γ229—whose vinculin genes had been disrupted (Coll et al., 1995). Normal F9 cells, cultured at low densities, appeared flat and epithelioid. Immunostaining of these cells for ZO-1 showed that this protein was discontinuously distributed at cell–cell boundaries (Fig. 8, *A* and *E*) as typically seen in fibroblasts; nevertheless, the ZO-1 signals were closely associated with vinculin (Fig. 8 *B*) as well as with E-cadherin at its apical borders (Fig. 8 *F*), as observed in epithelial cells. In the vinculin-null F9 cells that were less flat than the normal F9 cells, ZO-1 and E-cadherin were distributed in a pattern similar to that found in the normal cells (Fig. 8, *C*, *G* and *H*) despite the absence of vinculin (Fig. 8 *D*), although the ZO-1 pattern appeared more complicated in the mutant cells. As these cells grew and became more packed, we noted a dramatic difference in the ZO-1 distribution between the normal and vinculin-null cells. In normal cells, ZO-1 tended to be reorganized into honeycomb- or web-like networks on their top surfaces (Fig. 8, *I* and *M*). These ZO-1 signals colocalized with vinculin (Fig. 8 *J*), and also with the apical-most E-cadherin signals (Fig. 8 *N*). In contrast, the vinculin-null F9 cell layers rarely formed such closed web-like networks of ZO-1, maintaining the discontinuous ZO-1 pattern (Fig. 8, *K*, *O* and *P*), although they sometimes displayed partially closed organization of this molecule. The same results were obtained with both γ227 and γ229 cells. To confirm whether this mutant phenotype was directly brought about by the loss of vinculin, we further examined two sublines of γ229—R3 and R15—in which vinculin expression had been restored by virtue of vinculin cDNA transfection (Xu et al., 1998*b*). In both of the rescued lines, the web-like distribution of ZO-1, colocalizing with vinculin, was normally generated (Fig. 8, *Q* and *R*). The above ZO-1 networks were observed only at the top focal plane of the cell layers. These findings support the idea that vinculin is involved in organization of the apical-most junctions.

When we induced differentiation in the F9 lines by means of aggregation cultures with retinoic acid as described (Stephens et al., 1993), some of the resultant differentiated cells, likely visceral endoderm cells, exhibited a honeycomb-like organization of ZO-1, even in the absence of vinculin (data not shown). This finding suggests that vinculin may not be absolutely required for junctional organization in certain cell types or under certain physiological conditions.

Discussion

Cadherin-dependent and -independent Processes of TJ Organization

As previously reported (Watabe et al., 1994; Torres et al., 1997; van Hengel et al., 1997), in the absence of αE-cate-

Figure 8. Junctional organization in normal and vinculin-null F9 cells. (*A–H*) Low cell density. Cells (1×10^5) were inoculated on a collagen-coated coverslip placed in each 3.5-cm dish, and were cultured for 2 d. (*I–R*) High cell density. The above cultures were maintained for 4 d. (*A, B, E, F, I, J, M,* and *N*) Normal F9 cells. (*C, D, G, H, K, L, O,* and *P*) Vinculin-null γ229 cells. (*Q* and *R*) R15 cells that were isolated by transfection of γ229 with vinculin cDNA. ZO-1 was double-stained with vinculin (*A* and *B*; *C* and *D*; *I* and *J*; *K* and *L*; *Q* and *R*), and with E-cadherin (*E* and *F*; *G* and *H*; *M* and *N*; *O* and *P*). Note the web-like organization of ZO-1 in vinculin-positive cells cultured for 4 d. Such ZO-1 organization is prohibited in the absence of vinculin. Confocal images focused at the apical-most plane of cells are presented. zo, ZO-1; cad, E-cadherin; vin, vinculin. Bar, 20 μm.

nin, two components of the TJ—ZO-1 and occludin— could not be arranged into a honeycomb pattern along the apical cell–cell contact sites. Unexpectedly, however, our freeze-fracture studies revealed the presence of patchy TJ-like structures, even in the αE-catenin–deficient cells. We found that these cells were connected with filopodia at their apical regions. Presumably, these filopodial contacts provide sites for the punctate TJ formation. The role of the cadherin/αE-catenin system thus seems not to be initiation of TJ formation, but the assemblage of its components into the functional pattern. This notion is consistent with the previous findings that PKC activators can induce partial organization of the TJ in the absence of Ca^{2+} (Balda et al., 1993) or αE-catenin (van Hengel et al., 1997) that is required for normal cadherin activity, and that TJ formation is PKC-dependent whereas E-cadherin–mediated adhesion is not (Denisenko et al., 1994; Stuart and Nigam, 1995). Early studies suggest that desmosomal organi-

zation also depends on normal cadherin activity (Watabe et al., 1994; Lewis et al., 1994; Bornslaeger et al., 1996; Ruiz et al., 1996; Lewis et al., 1997; van Hengel et al., 1997). However, we frequently detected desmosomes in R2/7 cells, indicating that the formation of the desmosome is basically independent of the αE-catenin function, as is the case of the TJ.

The Role of αE-Catenin and Vinculin in Junctional Complex Assembly

In simple epithelia, TJ and ZA are located side by side. Actin filaments are accumulated not only in the ZA, but also in the TJ (Drenckhahn and Dermietzel, 1988). These structural arrangements suggest that the ZA is molecularly associated with the TJ through the underlying actin fibers or other components. It is possible that the ZA controls TJ organization through such a molecular linkage. If so, then how is αE-catenin involved in such processes?

By the domain analysis of αE-catenin, we found one important domain that is required for TJ organization: the 326–509 region. Without this domain, αE-catenin could not redistribute TJ components. The loss of this domain concomitantly abolished the colocalization of E-cadherin and αE-catenin with vinculin, suggesting that this region of αE-catenin may have the ability to interact with vinculin. In vitro binding assays indeed demonstrated that the head domain of vinculin, but not the tail domain, directly bound this 326–509 domain of αE-catenin. To examine the biological role of this αE-catenin-vinculin interaction, we constructed chimeric proteins and found that a polypeptide consisting of the NH_2-terminal portion of αE-catenin and the vinculin tail was sufficient for organization of the apical junctional complex. The vinculin head had no effect. We thus can envision a scheme in which vinculin binds αE-catenin via the head domain, and then acts for organization of the apical junctions via its tail domain. Vinculin is a well-known cytoskeletal protein associated with ZA, as well as with cell-substrate focal adhesion (Burridge and Feramisco, 1980; Geiger et al., 1980; Chen and Singer, 1982). It binds many cytoplasmic molecules, including α-actinin (Belkin and Koteliansky, 1987), paxillin (Turner et al., 1990; Wood et al., 1994), talin (Burridge and Mangeat, 1984), and actin (see below). In vinculin-deficient cells, cell-substrate adhesiveness and motility are altered (Samuels et al., 1993; Coll et al., 1995). Recent analysis of vinculin knockout mice revealed malformation in various tissues, including disarray of neuroepithelial cells (Xu et al., 1998a) that clearly indicated the importance of vinculin for multicellular organization. However, the epithelial phenotypes in these mutant mice remain to be analyzed in detail.

Our present results demonstrated that loss of vinculin impaired the TJ-like patterning of ZO-1 in F9 cells, supporting the above notion that vinculin was involved in apical junctional assembly. Although F9 cells may not be representative of mature epithelial cells, their apical ZO-1 pattern, observed in high cell density cultures, was reminiscent of that seen in typical simple epithelia, suggesting that F9 cells were capable of generating certain TJ-like junctions when their cultures were condensed. Importantly, vinculin deficiency in F9 cells only modestly affected their overall cell–cell adhesiveness (Tozeren et al.,

1998), and did not affect the accumulation of ZO-1 and E-cadherin into the fibroblast-type cell–cell contact sites that were seen in low cell density cultures. Thus, the defect in the vinculin-null cells was confined to the process of the weblike arrangement of ZO-1, suggesting that vinculin plays a specific role in the apical-most junctional assembly. This view is consistent with the apically restricted localization of vinculin, and also with our finding that the αE/vin-Tail induced only apical cell–cell adhesions. Vinculin is known to interact with actin filaments via its tail domain (Menkel et al., 1994; Johnson and Craig, 1995; Gilmore and Burridge, 1996). Based on this well-known property, we can imagine that vinculin may play a pivotal role in mediating the interaction of the cadherin/catenin complex with the apical actin bundles. Vinculin molecules associated with αE-catenin may function to recruit actin to the ZA, and assist its zipperlike extension along the apicolateral cell surfaces to establish closed belt–type junctions. TJs likely follow the extension of ZA via the above-proposed linkages between the two junctions so as to generate their own closed networks, although the real mechanisms remain to be elucidated. The honeycomb-type organization of ZO-1 was not completely excluded from the vinculin-null F9 cells, as we could detect such structures even in these cells under differentiation-induced conditions. This may not be surprising because TJs could be self-organized in a cadherin-independent manner, as discussed above. Under particular physiological conditions, the vinculin system may not be required for TJ assembly. However, there is no evidence that the junctions generated without vinculin are functionally and structurally normal.

In contradiction to the idea that vinculin interacts with actin bundles, we found that vinculin was not colocalized with the apical actin rings when αE-catenin was absent. This phenomenon can be explained by the ability of vinculin to undergo an intramolecular head-to-tail interaction, resulting in masking its COOH-terminal actin-binding site (Weekes et al., 1996; Johnson and Craig, 1995; Gilmore and Burridge, 1996). Vinculin may require binding to αE-catenin to expose its actin-binding site and to interact with the apical actin belt.

It was reported that vinculin is coimmunoprecipable with the E-cadherin/β-catenin complex from a line of αE-catenin–deficient cells (Hazan et al., 1997). That work speculated that vinculin bound β-catenin in place of αE-catenin. In our experimental materials, vinculin never colocalized with E-cadherin if αE-catenin was absent, suggesting no substantial association between the vinculin and the E-cadherin/β-catenin complex, at least at cell–cell contact sites under the αE-catenin–deficient conditions. We do not rule out the possibility that the E-cadherin/β-catenin complex might be associated with vinculin molecules localized at non cell–cell adhesion sites. Recently, the head domain of vinculin was shown to bind to α-catenin (Weiss et al., 1998), consistent with our findings. This work argued that the COOH-terminal region of α-catenin was involved in this binding. However, we found that the COOH-terminal region of α-catenin was not essential for the association of vinculin with E-cadherin or α-catenin both in vivo and in vitro. This discrepancy perhaps arose from technical differences between the two studies, and it must be settled in the future studies.

αE-catenin itself is known to interact with actin (Rimm et al., 1995). Then, why is the αE-catenin unable to use its own actin-binding sites for the apical junctional assembly? Vinculin might simply have a higher affinity for actin than for αE-catenin. Alternatively, the apical actin bundles might be associated with some molecules that specifically interact with vinculin; these molecules mediate the vinculin–actin interaction. If this mechanism is the case, αE-catenin should not be able to function in place of vinculin for organization of the ZA-TJ complex. αE-catenin was shown to be coimmunoprecipitated with α-actinin (Knudsen et al., 1995; Tsukatani et al., 1997), and its 325–394 domain was identified by the yeast two-hybrid method (Nieset et al., 1997) as a site binding α-actinin. Because of this reported property of α-actinin, this protein can be considered as another linker between the E-cadherin/αE-catenin complex and actin fibers. However, we found that αE/vinTail, not containing any identified α-actinin-binding sites, still could reorganize the ZO-1 distribution, whereas αE/vinHead with an α-actinin binding site on its vinculin moiety (Kroemker et al., 1994) failed to do so. These observations suggest that the α-actinin–αE-catenin interaction may not be required for the cadherin-dependent TJ assembly.

Functions of E-Cadherin and αE-Catenin in Nonapical Cell–Cell Junctions

In the lateral membrane below the ZA, the E-cadherin/αE-catenin complex appears to be free from vinculin. At these sites, the COOH-terminal domain of αE-catenin could directly interact with cortical actins, exerting some action on cadherin activity, as widely believed. The importance of the COOH-terminal domain in cadherin-mediated adhesion was previously demonstrated by use of fibroblastic cells (Nagafuchi et al., 1994) and pre-implantation mouse embryos (Torres et al., 1997). Consistently, DLD-1 cells lacking this domain were less adhesive than those with the full-length αE-catenin, and they could not perfectly organize the lateral cell association pattern. Furthermore, cells expressing αE/vinTail without the αE-catenin COOH terminus adhered to one another only by the apical junctions and desmosomes, suggesting that the COOH terminus is required for adhesion between the nonapical lateral membranes. Perhaps the internal 326–509 and COOH terminal domains have distinct functions. It is likely that the internal domain is specialized for ZA formation or ZA-TJ interaction, and the COOH terminus is critical for general cadherin-dependent adhesion at nonapical cell membranes.

Some additional information on E-cadherin activity was obtained from this study. E-cadherin was concentrated at cell–cell contact sites in the absence of αE-catenin, and the αE-catenin–deficient cells were able to aggregate to some extent in an E-cadherin–dependent manner, indicating that E-cadherin molecules undergo homophilic interactions without αE-catenin, as expected from previous in vitro (Brieher et al., 1996) as well as in vivo studies (Shimoyama et al., 1992; van Hengel et al., 1997). Some E-cadherin molecules were localized along the ZO-1/actin ring in the αE-catenin–deficient cells. These E-cadherin molecules could be the ones concentrated at filopodial contact sites as a result of their homophilic interaction.

In sum, our results suggest that αE-catenin regulates apical junctional assembly via binding to vinculin. It remains to be solved how generally this mechanism is used for junctional organization in different cell types. Closer analyses of cell–cell junction structures in different tissues of the vinculin-mutant mice (Xu et al., 1998a) should be helpful in addressing this question.

References

Balda, M.S., L. Gonzalez-Mariscal, K. Matter, M. Cereijido, and J.M. Anderson. 1993. Assembly of the tight junctions: the role of diacylglycerol. *J. Cell Biol.* 123:293–302.

Barth, A.I.M., I.S. Näthke, and W.J. Nelson. 1997. Cadherins, catenins and APC protein: interplay between cytoskeletal complexes and signaling pathways. *Curr. Opin. Cell Biol.* 9:683–690.

Belkin, A.M., and V.E. Koteliansky. 1987. Interaction of iodinated vinculin, metavinculin and alpha-actinin with cytoskeletal proteins. *FEBS Lett.* 220:291–294.

Boller, K., D. Vestweber, and R. Kemler. 1985. Cell adhesion molecule uvomorulin is localized in the intermediate junctions of adult intestinal epithelial cells. *J. Cell Biol.* 100:327–332.

Bornslaeger, E.A., C.M. Corcoran, T.S. Stappenbeck, and K.J. Green. 1996. Breaking the connection: displacement of the desmosomal plaque protein desmoplakin from cell-cell interfaces disrupts anchorage of intermediate filament bundles and alters intercellular junction assembly. *J. Cell Biol.* 134:985–1001.

Brieher, W.M., A.S. Yap, and B.M. Gumbiner. 1996. Lateral dimerization is required for the homophilic binding activity of C-cadherin. *J. Cell Biol.* 135:487–496.

Bullions, L.C., D.A. Notterman, L.S. Chung, and A.J. Levine. 1997. Expression of wild-type alpha-catenin protein in cells with a mutant alpha-catenin gene restores both growth regulation and tumor suppressor activities. *Mol. Cell Biol.* 17:4501–4508.

Burridge, K., and J. Feramisco. 1980. Microinjection and localization of a 130 K protein in living fibroblasts: a relationship to actin and fibronectin. *Cell.* 19:587–595.

Burridge, K., and P. Mangeat. 1984. An interaction between vinculin and talin. *Nature.* 308:744–746.

Buxton, R.S., and A.L. Magee. 1992. Structure and interactions of desmosomal and other cadherins. *Semin. Cell Biol.* 3:157–167.

Chen, W.T., and S.J. Singer. 1982. Immunoelectron microscopic studies of the sites of cell substratum and cell-cell contacts in cultured fibroblasts. *J. Cell Biol.* 95:205–222.

Coll, J.-L., A. Ben-Ze'ev, R.M. Ezzell, J.L.R. Fernandez, H. Baribault, R.G. Oshima, and E.D. Adamson. 1995. Targeted disruption of vinculin genes in F9 and embryonic stem cells changes cell morphology, adhesion, and locomotion. *Proc. Natl. Acad. Sci. USA.* 92:9161–9165.

Craig, S.W., and J.V. Pardo. 1979. Alpha-actinin localization in the junctional complex of intestinal epithelial cells. *J. Cell Biol.* 80:203–210.

Denisenko, N., P. Burighel, and S. Citi. 1994. Different effects of protein kinase inhibitors on the localization of junctional proteins at cell-cell contact sites. *J. Cell Sci.* 107:969–981.

Dexter, D.L., J.A. Barbosa, and P. Carabresi. 1979. *N,N*-dimethylformamide-induced alteration of cell culture characteristics and loss of tumorigenicity in cultured human colon carcinoma cells. *Cancer Res.* 39:1020–1025.

Drenckhahn, D., and R. Dermietzel. 1988. Organization of the actin filament cytoskeleton in the intestinal brush border: A quantitative and qualitative immunoelectron microscopy study. *J. Cell Biol.* 107:1037–1048.

Farquhar, M.G., and G.E. Palade. 1963. Junctional complexes in various epithelia. *J. Cell Biol.* 17:375–412.

Furuse, M., T. Hirase, M. Itoh, A. Nagafuchi, S. Yonemura, S. Tsukita, and S. Tsukita. 1993. Occludin: a novel integral membrane protein localizing at tight junctions. *J. Cell Biol.* 123:1777–1788.

Furuse, M., M. Itoh, T. Hirase, A. Nagafuchi, S. Yonemura, S. Tsukita, and S. Tsu-

kita. 1994. Direct association of occludin with ZO-1 and its possible involvement in the localization of occludin at tight junctions. *J. Cell Biol*. 127:1617–1626.

Geiger, B., K.T. Tokuyasu, and S.J. Singer. 1979. Immunocytochemical localization of α-actinin in intestinal epithelial cells. *Proc. Natl. Acad. Sci. USA*. 76:2833–2837.

Geiger, B., K.T. Tokuyasu, A.H. Dutton, and S.J. Singer. 1980. Vinculin, an intracellular protein localized at specialized sites where microfilament bundles terminate at cell membranes. *Proc. Natl. Acad. Sci. USA*. 77:4127–4131.

Geiger, B., A.H. Dutton, K.T. Tokuyasu, and S.J. Singer. 1981. Immunoelectron microscope studies of membrane-microfilament interactions: Distributions of α-actinin, tropomyosin, and vinculin in intestinal epithelial brush border and chicken gizzard smooth muscle cells. *J. Cell Biol*. 91:614–628.

Gilmore, A.P., and K. Burridge. 1996. Regulation of vinculin binding to talin and actin by phosphatidyl-inositol-4-5-bisphosphate. *Nature*. 381:531–535.

Gritz, L., and J. Davies. 1983. Plasmid-encoded hygromycin B resistance: the sequence of hygromycin B phosphotransferase gene and its expression in *Escherichia coli* and *Saccharomyces cerevisiae*. *Gene*. 25:179–188.

Gumbiner, B., and K. Simons. 1986. A functional assay for proteins involved in establishing an epithelial occluding barrier: identification of a uvomorulin like polypeptide. *J. Cell Biol*. 102:457–468.

Gumbiner, B., B. Stevenson, and A. Grimaldi. 1988. The role of the cell adhesion molecule uvomorulin in the formation and maintenance of the epithelial junctional complex. *J. Cell Biol*. 107:1575–1587.

Hazan, R.B., L. Kang, S. Roel, P.I. Borgen, and D.L. Rimm. 1997. Vinculin is associated with the E-cadherin adhesion complex. *J. Biol. Chem*. 272:32448–32453.

Herrenknecht, K., M. Ozawa, C. Eckerskorn, F. Lottspeich, M. Lenter, and R. Kemler. 1991. The uvomorulin-anchorage protein α-catenin is a vinculin homologue. *Proc. Natl. Acad. Sci. USA*. 88:9156–9160.

Hirano, S., N. Kimoto, Y. Shimoyama, S. Hirohashi, and M. Takeichi. 1992. Identification of a neural α-catenin as a key regulator of cadherin function and multicellular organization. *Cell*. 70:293–301.

Itoh, M., A. Nagafuchi, S. Moroi, and S. Tsukita. 1997. Involvement of ZO-1 in cadherin-based cell adhesion through its direct binding to α-catenin and actin filaments. *J. Cell Biol*. 138:181–192.

Johnson, R.P., and S.W. Craig. 1995. F-actin binding site masked by the intramolecular association of vinculin head and tail domains. *Nature*. 373:261–264.

Knudsen, K.A., A.P. Soler, K.R. Johnson, and M.J. Wheelock. 1995. Interaction of α-actinin with the cadherin/catenin cell-cell adhesion complex via α-catenin. *J. Cell Biol*. 130:67–77.

Kroemker, M.R., A.H. Rudiger, B.M. Jockusch, and M. Rudiger. 1994. Intramolecular interactions in vinculin control alpha-actinin binding to the vinculin head. *FEBS Lett*. 355:259–262.

Lewis, J.E., P.J. Jensen, and M.J. Wheelock. 1994. Cadherin function is required for human keratinocytes to assemble desmosomes and stratify in response to calcium. *J. Invest. Dermatol*. 102:870–877.

Lewis, J.E., J.K. Wahl III, K.M. Sass, P.J. Jensen, K.R. Johnson, and M.J. Wheelock. 1997. Cross-talk between adherens junctions and desmosomes depends on plakoglobin. *J. Cell Biol*. 136:919–934.

Mandai, K., H. Nakanishi, A. Satoh, H. Obaishi, M. Wada, H. Nishioka, M. Itoh, A. Mizoguchi, T. Aoki, T. Fujimoto, et al. 1997. Afadin: a novel actin filament-binding protein with one PDZ domain localized at cadherin-based cell-to-cell adherens junction. *J. Cell Biol*. 139:517–528.

Menkel, A.R., M. Kroemker, P. Bubeck, M. Ronsiek, G. Nikolai, and B.M. Jockusch. 1994. Characterization of an F-actin-binding domain in the cytoskeletal protein vinculin. *J. Cell Biol*. 126:1231–1240.

Molony, L., and K. Burridge. 1985. Molecular shape and self-association of vinculin and metavinculin. *J. Cell Biochem*. 29:31–36.

Nagafuchi, A., M. Takeichi, and S. Tsukita. 1991. The 102-kd cadherin-associated protein: Similarity to vinculin and posttranscriptional regulation of expression. *Cell*. 65:849–857.

Nagafuchi, A., and S. Tsukita. 1994. The loss of the expression of α-catenin, the 102 kD cadherin associated protein, in central nervous tissues during development. *Dev. Growth Differ*. 36:59–71.

Nagafuchi, A., S. Ishihara, and S. Tsukita. 1994. The roles of catenins in the cadherin-mediated cell adhesion: Functional analysis of E-cadherin-α-catenin fusion molecules. *J. Cell Biol*. 127:235–245.

Nieset, J.E., A.R. Redfield, F. Jin, K.A. Knudsen, K.R. Johnson, and M.J. Wheelock. 1997. Characterization of the interactions of α-catenin with α-actinin and β-catenin/plakoglobin. *J. Cell Sci*. 110:1013–1022.

Obama, H., and M. Ozawa. 1997. Identification of the domain of α-catenin involved in its association with β-catenin and plakoglobin (γ-catenin). *J. Biol. Chem*. 272:11020–11020.

Rajasekaran, A.K., M. Hojo, T. Huima, and E. Rodriguez-Boulan. 1996. Catenins and zonula occludens-1 form a complex during early stages in the assembly of tight junctions. *J. Cell Biol*. 132:451–463.

Rimm, D.L., E.R. Koslov, P. Kebriaei, C.D. Cianci, and J.S. Morrow. 1995. α1(E)-catenin is an actin-binding and -bundling protein mediating the attachment of F-actin to the membrane adhesion complex. *Proc. Natl. Acad. Sci. USA*. 92:8813–8817.

Ruiz, P., V. Brinkmann, B. Ledermann, M. Behrend, C. Grund, C. Thalhammer, F. Vogel, C. Birchmeier, U. Gunthert, W.W. Franke, and W. Birchmeier. 1996. Targeted mutation of plakoglobin in mice reveals essential functions of desmosomes in the embryonic heart. *J. Cell Biol*. 135:215–225.

Saitou, M., Y. Ando-Akatsuka, M. Itoh, M. Furuse, J. Inazawa, K. Fujimoto,

and S. Tsukita. 1997. Mammalian occludin in epithelial cells: its expression and subcellular distribution. *Eur. J. Cell Biol*. 73:222–231.

Samuels, M., R.M. Ezzell, T.J. Cardozo, D.R. Critchley, J.-L. Coll, and E.D. Adamson. 1993. Expression of chicken vinculin complements the adhesion-defective phenotype of a mutant mouse F9 embryonal carcinoma cell. *J. Cell Biol*. 121:909–921.

Sehgal, R.N., B.M. Gumbiner, and L.F. Reichardt. 1997. Antagonism of cell adhesion by an α-catenin mutant, and of the Wnt-signaling pathway by α-catenin in *Xenopus* embryos. *J. Cell Biol*. 139:1033–1046.

Shibamoto, S., M. Hayakawa, K. Takeuchi, T. Hori, N. Oku, K. Miyazawa, N. Kitamura, M. Takeichi, and F. Ito. 1994. Tyrosine phosphorylation of β-catenin and plakoglobin enhanced by hepatocyte growth factor and epidermal growth factor in human carcinoma cells. *Cell Adhesion Commun*. 1:295–305.

Shimoyama, Y., S. Hirohashi, S. Hirano, M. Noguchi, Y. Shimosato, M. Takeichi, and O. Abe. 1989. Cadherin cell-adhesion molecules in human epithelial tissues and carcinomas. *Cancer Res*. 49:2128–2133.

Shimoyama, Y., A. Nagafuchi, S. Fujita, M. Gotoh, M. Takeichi, S. Tsukita, and S. Hirohashi. 1992. Cadherin dysfunction in a human cancer cell line: possible involvement of loss of δ-catenin expression in reduced cell-cell adhesiveness. *Cancer Res*. 52:1–5.

Shirayoshi, Y., A. Nose, K. Iwasaki, and M. Takeichi. 1986. N-linked oligosaccharides are not involved in the formation of a cell-cell binding glycoprotein E-cadherin. *Cell Struct. Funct*. 11:245–252.

Stephens, L.E., J.E. Sonne, M.L. Fitzgerald, and C.H. Damsky. 1993. Targeted deletion of β1 integrins in F9 embryonal carcinoma cells affects morphological differentiation but not tissue specific gene expression. *J. Cell Biol*. 123:1607–1620.

Stuart, R.O., and S.K. Nigam. 1995. Regulated assembly of tight junctions by protein kinase C. *Proc. Natl. Acad. Sci. USA*. 92:6072–6076.

Sugden, B., K. Marsh, and J. Yates. 1985. A vector theat replicates as a plasmid and can be efficiently selected in B-lymphoblasts transformed by Epstein-Barr virus. *Mol. Cell Biol*. 5:410–413.

Takeichi, M. 1977. Functional correlation between cell adhesive properties and some cell surface proteins. *J. Cell Biol*. 75:464–474.

Takeichi, M. 1988. The cadherins: Cell-cell adhesion molecules controlling animal morphogenesis. *Development*. 102:639–655.

Torres, M., A. Stoykova, O. Huber, K. Chowdhury, P. Bonaldo, A. Mansouri, S. Butz, R. Kemler, and P. Gruss. 1997. An αE-catenin gene trap mutation defined its function in preimplantation development. *Proc. Natl. Acad. Sci. USA*. 94:901–906.

Tozeren, A., S. Wu, B. Hoxter, W. Xu, E.D. Adamson, and S.W. Byers. 1998. Vinculin and cell-cell adhesion. *Cell Adhesion Commun*. 5:49–59.

Tsukatani, Y., K. Suzuki, and K. Takahashi. 1997. Loss of density-dependent growth inhibition and dissociation of α-catenin from E-cadherin. *J. Cell. Physiol*. 173:54–63.

Turner, C.E., J.R. Glenney, Jr., and K. Burridge. 1990. Paxillin: a new vinculin-binding protein present in focal adhesions. *J. Cell Biol*. 111:1059–1068.

Uchida, N., Y. Honjo, K.R. Johnson, M.J. Wheelock, and M. Takeichi. 1996. The catenin/cadherin adhesion system is localized in synaptic junctions bordering transmitter release zones. *J. Cell Biol*. 135:767–779.

van Hengel, J., L. Gohon, E. Bruyneel, S. Vermeulen, M. Cornelissen, M. Mareel, and F. van Roy. 1997. Protein kinase C activation upregulates intercellular adhesion of α-catenin-negative human colon cancer cell variants via induction of desmosomes. *J. Cell Biol*. 137:1103–1116.

Vermeulen, S.J., E.A. Bruyneel, M.E. Bracke, G.K. De Bruyne, K.M. Vennekens, K.L. Vleminckx, G.J. Berx, F.M. van Roy, and M.M. Mareel. 1995. Transition from the noninvasive to the invasive phenotype and loss of alpha-catenin in human colon cancer cells. *Cancer Res*. 55:4722–4728.

Watabe, M., A. Nagafuchi, S. Tsukita, and M. Takeichi. 1994. Induction of polarized cell-cell association and retardation of growth by activation of the E-cadherin-catenin adhesion system in a dispersed carcinoma line. *J. Cell Biol*. 127:247–256.

Weekes, J., S.T. Barry, and D.R. Critchley. 1996. Acidic phospholipids inhibit the intramolecular association between the N- and C-terminal regions of vinculin, exposing actin-binding and protein kinase C phosphorylation sites. *Biochem. J*. 314:827–832.

Weiss, E.E., M. Kroemker, A.-H. Rudiger, and M. Rudiger. 1998. Vinculin is part of the cadherin-catenin junctional complex: complex formation between α-catenin and vinculin. *J. Cell Biol*. 141:755–764.

Wood, C.K., C.E. Turner, P. Jackson, and D.R. Critchley. 1994. Characterization of the paxillin-binding site and the C-terminal focal adhesion targeting sequence in vinculin. *J. Cell Sci*. 107:709–717.

Xu, W., H. Baribault, and E.D. Adamson. 1998*a*. Vinculin knockout results in heart and brain defects during embryonic development. *Development*. 125:327–337.

Xu, W., J.-L. Coll, and E.D. Adamson. 1998*b*. Rescue of the mutant phenotype by reexpression of full-length vinculin in null F9 cells; effects on cell locomotion by domain deleted vinculin. *J. Cell Sci*. 111:1535–1544.

Yamamoto, T., N. Harada, K. Kano, S. Taya, E. Canaani, Y. Matsuura, A. Mizoguchi, C. Ide, and K. Kaibuchi. 1997. The ras target AF-6 interacts with ZO-1 and serves as a peripheral component of tight junctions in epithelial cells. *J. Cell Biol*. 139:785–795.

Yonemura, S., M. Itoh, A. Nagafuchi, and S. Tsukita. 1995. Cell-to-cell adherens junction formation and actin filament organization: similarities and differences between non-polarized fibroblasts and polarized epithelial cells. *J. Cell Sci*. 108:127–142.